Prediction of effective thermal conductivity of a suspension of core-shell particles using asymptotic homogenization ⊘

Karthiban A (கார்த்திபன் அ) ⓘ ; Easwar M K (ஈஸ்வர் ம கு) ⓘ ;
A. Arockiarajan (அ ஆரோக்கியராஜன்) ⓘ ; Anubhab Roy (অনুভব রায়) ✉ ⓘ

Check for updates

View Online   Export Citation

Articles You May Be Interested In

A multiscale approach to predict the effective conductivity of a suspension using the asymptotic homogenization method

Physics of Fluids (June 2022)

Large deformation of electro-magneto-thermo-elastic (EMTE) bilaminates

AIP Conf. Proc. (September 2024)

Reply to "Comment on 'Finite-element modeling method for the study of dielectric relaxation at high frequencies of heterostructures made of multilayered particle'" [J. Appl. Phys. 102, 124107 (2007)]

Journal of Applied Physics (November 2008)

Prediction of effective thermal conductivity of a suspension of core-shell particles using asymptotic homogenization

View Online   Export Citation   CrossMark

Karthiban A (கார்த்திபன் அ),[1] (iD) Easwar M K (ஈஸ்வர் ம கு),[2] (iD) A. Arockiarajan (அ ஆரோக்கியராஜன்),[1,3] (iD)
and Anubhab Roy (অনুভব রায়)[1,a] (iD)

AFFILIATIONS

[1]Department of Applied Mechanics, Indian Institute of Technology Madras, Chennai, Tamil Nadu, India
[2]SankhyaSutra Labs Ltd., Bengaluru, India
[3]Centre of Excellence in Ceramics Technologies for Futuristic Mobility, Indian Institute of Technology Madras (IIT Madras),
 Chennai, Tamil Nadu, India

[a]Author to whom correspondence should be addressed: anubhab@iitm.ac.in

ABSTRACT

This study presents the implementation of the asymptotic homogenization method (AHM) to predict the effective thermal conductivity of suspensions featuring core-shell particles. The AHM leverages the significant difference in scales between macroscopic and microscopic structures, making it possible to model the domain at multiple scales by capturing the influence of microscopic inclusions under macroscopic loading conditions on the domain. The study begins by deriving an analytical formulation for the thermal conductivity problem of core-shell composites, using a multiscale asymptotic expansion, followed by developing a finite element model to solve the unit cell problem. The results for core-shell inclusions are validated against known analytical solutions for different volume fractions. At low inclusion volume fractions, the numerical predictions closely match the effective medium approximations. However, at semi-dilute packing fractions, the AHM shows superior accuracy, aligning more closely with the experimental and analytical results. The study reveals that the effective thermal conductivity of the three-component composite is influenced by the volume fractions of the core and shell, the thermal conductivities of the core, shell, and matrix, as well as the spatial distribution of inclusions. The proposed AHM method coupled with finite element analysis offers a generalized approach to predict effective thermal or electrical conductivity.

Published under an exclusive license by AIP Publishing. https://doi.org/10.1063/5.0246385

I. INTRODUCTION

Particle-reinforced composites are widely used in various engineering sectors, ranging from aerospace[1] to energy[2] and electronics.[3] Despite their extensive applications, accurately computing and predicting the effective behavior of these materials remains a significant challenge. The enhancement of the effective suspension properties due to the presence of these inclusions applies to various mechanical and transport properties, such as elasticity, diffusivity, and thermal conductivity. Interactions between the different constituents in composite materials occur on a length scale much smaller than the characteristic length scale of the heterogeneous medium. Multiscale models capitalize on such differences in length scales to compute the effective properties of the medium, using homogenization techniques which include Mori–Tanaka,[4] self-consistent approach,[5] and asymptotic homogenization[6,7] to name a few. These methods are widely used in elastic and

transport problems to determine the effective property, particularly at dilute concentrations ($\phi < 0.1$) of inclusion.

Maxwell[8] made the earliest attempt to calculate effective conductivity considering non-interacting spherical inclusions with volume fraction ϕ and conductivity κ_{inc}, embedded in an infinite matrix with conductivity κ_m. The effective conductivity κ_{eff}, is then expressed as a function of the conductivities and the volume fraction. However, this expression is only accurate up to $\mathcal{O}(\phi)$ and is valid only at dilute volume fractions. On the other hand, in the limit of close-packing (ϕ_{max}), analytical progress has been achieved by examining interactions between neighboring particles. Keller[9] pioneered the approach of investigating interparticle interactions and provided analytical expressions for the conductivity of spherical inclusions within a cubic matrix near maximum packing fractions. His work laid the foundation for further studies on effective thermal conductivity in two-component

11 January 2025 07:12:38

composites. Subsequent work by Batchelor and O'Brien[10] addressed complex double asymptotic limits involving large but finite inclusion conductivity and small gaps between inclusions near the maximum packing fraction. They calculated the effective conductivity by considering the dipole strength of spherical particles in contact with each other. McPhedran and McKenzie[11] further expanded on this work by devising a multipole expansion method to predict the conductivity of systems arranged in a simple cubic structure, achieving high accuracy even for close-packed spheres. At this close-packing limit, Sangani and Acrivos[12] contributed by modifying Zuzovsky and Brenner's[13] methodology to solve a set of linear equations, allowing for the computation of effective conductivity for spherical inclusions.

Several investigations have been conducted to predict the effective properties of suspension of homogeneous inclusions over a wide range of inclusion volume fractions; however, they are rarely compared with known asymptotic limits in the dense packing regimes. The work of Easwar et al.,[14] employing the asymptotic homogenization method (AHM) to predict effective properties, is notable for its ability to accurately capture the behavior of suspension in both dilute and near-packing conditions. AHM leverages scale separation to incorporate microstructural effects. It systematically incorporates interparticle interactions, providing accurate predictions at near-packing limits, aligning with the asymptotic estimates[9–12] in that regime. These rigorous comparisons with the analytical results make AHM a superior framework for analyzing composite systems, particularly when particle interactions dominate as systems approach maximum packing.

While traditional two-component heterogeneous media, consisting of solid inclusions embedded in a continuous matrix, have been extensively studied and modeled, recent advancements in materials science and manufacturing techniques have led to the development of hybrid particles, such as core-shell structures. Core-shell particles (CSP) consist of two materials, forming the inner core and the outer shell. This design allows for enhanced customization of a composite's effective properties, surpassing the capabilities of either material alone. These hybrid particles have found applications across various fields, including thermal energy storage systems,[15] thermal insulation for enhancing energy efficiency in civil structures,[16] and as functional additives in polymers to improve mechanical and thermal properties.[17] However, the interaction between the core and shell materials and their combined effect on the surrounding matrix introduces complexity in predicting the effective thermal conductivity (ETC) of composites reinforced with core-shell particles.

This study aims to (1) review current models for predicting the effective thermal conductivity of composites containing spherical CSP, (2) develop a generalized method that uses the robustness of AHM with the effectiveness of finite element (FE) solutions to predict effective properties across various parameters, and (3) evaluate the influence of volume fraction, conductivity ratios, and particle interactions on the effective thermal conductivity of these composites.

II. CORE-SHELL PARTICLE REINFORCED COMPOSITES: EXISTING MODELS AND APPROACHES

Maxwell's method can be extended to include systems of spherical inclusions with contact resistance[18] and core-shell inclusions[19] as shown below. As we advance, this adaptation will be called the extended Maxwell method.
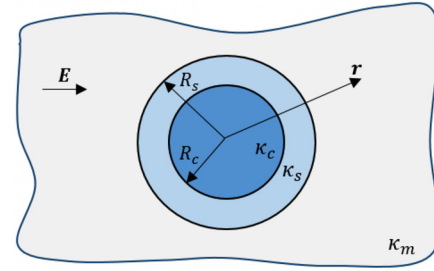

FIG. 1. A single core-shell particle in infinite medium.

A single core-shell particle embedded in an infinite matrix is considered (Fig. 1). The core, shell and matrix are represented by the subscripts c, s, and m respectively. The thermal conductivity coefficients of these phases are denoted as κ_c, κ_s, and κ_m. The core and outer shell have radii R_c and R_s, and their volume fractions are represented by ϕ_c and ϕ_s. The combined volume fraction of the core and shell is denoted as ϕ_{csp}.

Let r be the position vector, and T be the temperature distribution function. A constant temperature gradient E is applied at infinity and the distribution of temperatures in the heterogeneous media is given by

$$T_c = C_c(\boldsymbol{E}.\boldsymbol{r}), \quad r \leq R_c, \tag{1}$$

$$T_s = \left(S_1 + \frac{S_2}{r^3}\right)(\boldsymbol{E}.\boldsymbol{r}), \quad R_c \leq r \leq R_s, \tag{2}$$

$$T_m = \left(1 + \frac{C_m}{r^3}\right)(\boldsymbol{E}.\boldsymbol{r}), \quad r \geq R_s, \tag{3}$$

where

$$E = -\nabla \cdot \mathbf{T}, \tag{4}$$

where C_c, S_1, S_2, and C_m are unknown coefficients. By applying the boundary conditions, we solved the heat equation for the unknowns, thereby obtaining the temperature distribution. Subsequently, following the Maxwell analogy, which posits that a homogeneous sphere with an equivalent radius R_{eq} induces the same perturbation in the far field as a well-mixed cluster of N spherical inclusions, we get

$$\kappa_{eff} = \kappa_m \left(\frac{1 - 2\phi_{csp}\lambda}{1 + \phi_{csp}\lambda}\right), \tag{5}$$

where

$$\lambda = \left(\frac{(1-\beta)(\alpha + 2\beta) + \frac{R_c^3}{R_s^3}(1 + 2\beta)(\beta - \alpha)}{(\alpha + 2\beta)(2 + \beta) + 2\frac{R_c^3}{R_s^3}(1 - \beta)(\beta - \alpha)}\right),$$

$$\alpha = \frac{k_c}{k_s}, \quad \beta = \frac{k_s}{k_m}, \quad \phi_{csp} = N\frac{R_s^3}{R_{eq}^3}. \tag{6}$$

The derived expression is accurate only up to $\mathcal{O}(\phi)$ since this approach does not incorporate microstructural information beyond the volume fraction. Later, Herve[20] investigated a multilayered isotropic spherical inclusion surrounded by an infinite matrix, introducing a multistage homogenization technique. This process homogenizes the core and shell into an equivalent inclusion with an effective

11 January 2025 07:12:38

conductivity (κ_{csp}), treated that as a single inclusion in an infinite medium for further homogenization. Park et al.[21] also developed a model using a similar approach, based on the Mori–Tanaka[4] method, which yielded an expression similar to that of Herve's model for a two-component core-shell composite. Although these models[19–21] are derived using different approaches, the results predicted are similar to each other and the results obtained were valid for dilute volume fractions.

Meanwhile, Woodside and Messmer[22] used Lichtenecker's[23] model, also known as the geometric mean method, to compute the ETC of three-component composites. This model suggests that if the thermal conductivity of either the core or the shell vanishes, the effective conductivity (κ_{eff}) would also be zero. However, this prediction is not accurate because heat conduction could still occur through the continuous matrix material. The Brailsford and Major model is another prevalent ETC model for composites reinforced with core-shell particles. Brailsford and Major[24] extended the two-component model to include monodisperse core-shell particles randomly distributed in a continuous matrix. However, Ngo and Truong[25] and Thiele et al.[26] have demonstrated both Lichtenecker's[23] and Brailsford and Major's[24] models to be unable to accurately predict the effective conductivity when there is a significant difference in the magnitudes of the conductivities of the constituent phases.

Felske's model,[27] derived using the self-consistent field approximation, is considered effective in predicting the properties of core-shell composites.[25,26] However, when the shell material is absent ($\phi_s = 0$), Felske's model reduces to a form similar to Maxwell's model. This suggests that Felske's model might underestimate the effective thermal conductivity (ETC) of core-shell composites when the volume fraction of core-shell particles (ϕ_{csp}) is sufficiently high. Additionally, Pal[28] noted that Felske's model accurately describes the effective thermal conductivity when $\phi_{csp} \leq 0.2$.

Further studies were conducted to predict the effective properties of composites with core-shell inclusions across the entire spectrum of volume fractions. In one of the earlier studies, Lu and Song[29] extended the work of Chiew and Glandt,[30] providing a general expression for the effective conductivity of coated inclusions while considering the effect of interparticle interactions. They evaluated the pair interaction between neighboring particles by solving a boundary value problem concerning two coated spheres. The resulting model achieved $\mathcal{O}(\phi^2)$ accuracy, remaining valid even at non-dilute volume fractions.

Pal[28] developed an implicit model to estimate the effective thermal conductivity of three-component composites, featuring monodisperse core-shell particles randomly dispersed in a continuous matrix. Employing the differential effective medium approach, this model considered the maximum packing limit of the inclusions. While the predictions aligned well with experimental data for 13 different samples of two-phase media, in the case of three-phase media, significant differences in the orders of magnitude of thermal conductivity coefficients led to an overstatement of the effective conductivity of the composite.

Following this, numerical techniques were employed to predict the homogenized macroscale properties of composites. Thiele et al.[26] and Shen and Zhou[31] utilized finite element methods for homogenizing core-shell composites. In addition, several authors conducted experimental studies[32–38] to determine the effective conductivity. The combined data from these diverse investigations are illustrated in Fig. 2, offering a comprehensive overview of the methods used to calculate and predict the effective thermal conductivity of core-shell composites at the macroscale. Despite the numerous contributions from
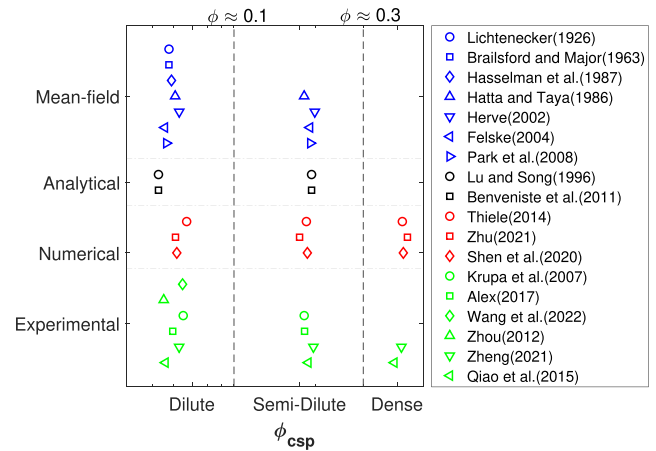

FIG. 2. Different methods from literature to predict effective thermal conductivity of CSP composites: mean field, analytical, numerical, and experimental approaches and their applicability across ϕ_{csp}. The volume fraction range is approximately split into three regimes: dilute (up to $\phi \approx 0.1$), semi-dilute (up to $\phi \approx 0.1$), and dense ($\phi > 0.3$), based on a simple cubic lattice approximation.).

various authors over the years, these models show significant differences among themselves. Therefore, there is uncertainty as to which model is the most appropriate and accurate. This uncertainty highlights the need for a more generalized method to predict the effective conductivity of composites with core-shell inclusions, regardless of the inclusion's volume fraction and conductivity ratios. Therefore, this work aims to provide a generalized method for predicting effective conductivity using the asymptotic homogenization method.

The asymptotic homogenization method (AHM)[6,50,51] exploits the sharp separation between the microscale and macroscale to decouple spatial variations and employs asymptotic expansions of the fields. Under the assumption of periodicity in the microstructure, this approach yields a set of effective governing equations that describe the macroscale mechanics of the heterogeneous material. A detailed review of AHM can be found in these articles.[52,53] Many authors have used AHM to predict effective properties for multifunctional layered composite materials[54–56] and have validated them against existing analytical expressions. In a recent work,[49] the accuracy of the AHM was compared with that of the representative volume element method in thermal composites, emphasizing efficacy of AHM. Although the derivations required to find the effective property expression are mathematically extensive, the use of FEM helps simplify the solving procedure. Such solving schemes have been adopted,[46–48] and the accuracy of the results obtained has been verified.

Effective medium models, such as the extended Maxwell model, accurately predict effective properties in dilute packing conditions but fail to capture interparticle interactions at semi-dilute and dense volume fractions. Lu and Song[29] provide a model that predicts effective conductivity well up to semi-dilute packing fractions. However, the available expressions are implicit functions of the volume ratio of core and shell, conductivity ratio, and volume fractions of inclusions, making it mathematically challenging to derive a closed-form solution for new combinations of these ratios. Finite element modeling using both unit cell and representative volume element (RVE) approaches offers an alternative to effective medium models for predicting the effective properties of composites. The

TABLE I. Overview of literature survey.

Domain	Literature	Remarks	Limitations
Mean-field methods	Maxwell,[8] Felske,[27] Hatta and Taya,[39] Herve,[20] Park et al.[21]	Single coated inclusion in an infinite matrix space	Applicable only at dilute volume fractions
Analytical estimates	Keller,[9] Batchelor and O'Brien,[10] McPhedran and McKenzie,[11] Sangani and Acrivos,[12] Bonnecaze and Brady[40]	Spherical inclusions	Assumes periodic arrangement at dense packing; deriving closed-form solutions for varying spatial distributions requires extensive mathematical rigor
	Lu and Song,[29] Nan et al.,[41] Benveniste and Milton,[42] Cheng and Torquato[43]	Spherical inclusions with interfacial resistance and coatings	
Numerical methods	Thiele et al.,[26] Zhu et al.,[44] Shen and Zhou[31]	Core-shell inclusions in a unit cell	Conducted at macroscale; focuses on macroscopic variations only
Asymptotic homogenization	Torquato,[45] Andreassen and Andreasen,[46] Fantoni et al.,[47] Dutra et al.,[48] Lee and Lee[49]	Application of AHM in predicting effective transport coefficients	Requires significant scale separation between inclusions and macroscale for accurate results

unit cell model employs a single, repeating unit cell to represent the composite material, and assumes periodic boundary conditions.[57] In contrast, the RVE model uses a representative sample of the microstructure, making it suitable for heterogeneous and complex materials. However, this approach is computationally intensive and scale-dependent, as the model must be large enough to accurately capture the macroscale features of the material.[58] A comparative summary of these methods and their limitations is provided in Table I for reference.

Therefore, to predict the effective conductivity across the complete range of packing fractions and capture interparticle interactions near maximum packing fractions, we propose the present method. This method combines the robustness of the AHM with the efficiency of FEM to predict the effective conductivity of core-shell composites.

The multiscale formulation for the effective conductivity problem is derived in Sec. III A, followed by numerical methodology in Sec. III B. In Sec. IV A, the proposed methodology is benchmarked against known analytical results for homogeneous spherical inclusions, and then the study is extended to include CSP inclusions in Sec. IV B.

III. MULTISCALE MODELLING

In this work, we investigate composite materials with periodic arrangement, thus facilitating the application of periodic homogenization. It is, therefore, assumed that the composite is composed of many repeating unit cells, as shown in Fig. 3, whose length scale is well separated from the macroscopic structure. The unit cell determines material properties at the microstructure level, significantly influencing the material's macroscopic behavior.

As shown in Fig. 4, we consider a unit cell with inclusion of CSP in continuous media. The interface between the different phases within the composite is considered perfect (without any interface effects). Since the material is composed of many repeating unit cells, the associated material properties within each unit cell will recur over a constant length Y, termed as the periodicity of the material. In a heterogeneous

domain Ω having a periodic structure, any physical quantity ψ, demonstrates the following property:

$$\psi(\mathbf{x} + \mathbf{Y}) = \psi(\mathbf{x}) \quad \forall \mathbf{x} \quad \text{and} \quad \forall (\mathbf{x}+\mathbf{Y}) \in \Omega, \qquad (7)$$

where $\mathbf{x}$ is the position vector. Based on these assumptions and the existence of two distinguishable length scales, the effective properties of the heterogeneous media could be predicted by solving a finite number of unit cell problems.

A. Asymptotic homogenization method

If we consider a coordinate system in which the global coordinate vector $\boldsymbol{x}$ corresponds to the macroscopic structure, and the stretched local coordinate vector $\boldsymbol{y}$ represents the microscopic unit cell, then the two coordinate systems are related by a scale separation parameter ε, as

$$y_i = \frac{x_i}{\varepsilon}, \quad \varepsilon \ll 1. \qquad (8)$$

The slow or global variable, $\mathbf{x}$, captures variations at the macroscale $[\mathcal{O}(1)]$; variations at the microscopic length scale $[\mathcal{O}(\varepsilon)]$, which scales
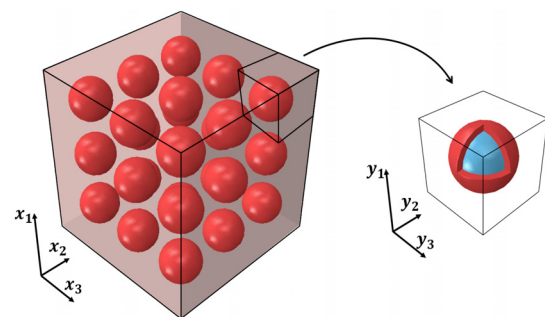

FIG. 3. Continuous media with periodic inclusion and the corresponding unit cell.
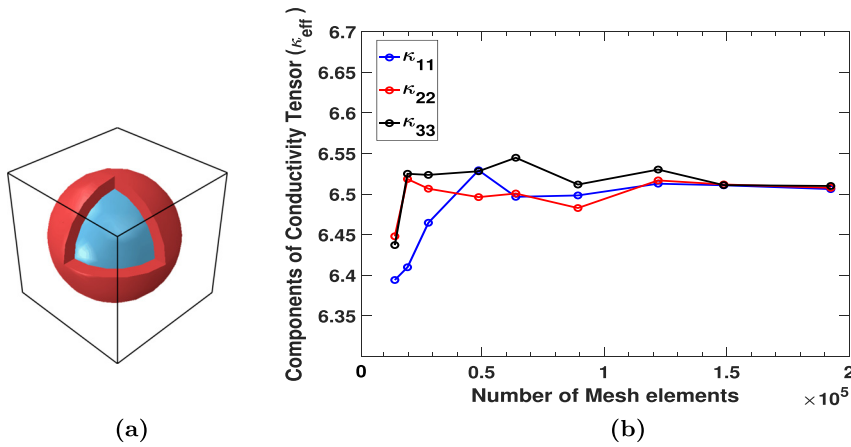
the macroscopic length scale by $1/\varepsilon$, are captured by the finer scale $\mathbf{y}$, as defined in Eq. (8). As the microstructural parameter ε approaches zero, the fields under consideration converge toward a homogeneous macroscopic solution.

Now, a thermal conductivity problem within a heterogeneous domain Ω is considered, with the governing equations defined as the following:

1. Balance equation:

$$Q_{i,i}^{\varepsilon}(\mathbf{x}) = 0 \quad \text{in} \quad \Omega, \tag{9}$$

2. Constitutive relation:

$$Q_i^{\varepsilon}(\mathbf{x}) = \kappa_{ij}^{\varepsilon}(\mathbf{x})E_j^{\varepsilon}(\mathbf{x}) \quad \text{in} \quad \Omega, \tag{10}$$

3. Temperature gradient:

$$E_i^{\varepsilon}(\mathbf{x}) = -T_{,i}^{\varepsilon}(\mathbf{x}) \quad \text{in} \quad \Omega, \tag{11}$$

4. Boundary conditions and jumps:

$$[\![Q_i^{\varepsilon} n_i]\!] = 0 \quad \text{on the interface}, \tag{12}$$
$$[\![T^{\varepsilon}]\!] = 0 \quad \text{on the interface}, \tag{13}$$

where $Q_i(\mathbf{x})$ denotes heat flux, $E_i(\mathbf{x})$-the temperature gradient, $\kappa_{ij}(\mathbf{x})$-the thermal conductivity tensor, T is the temperature potential, and the superscript ε denote that the macroscopic quantities that have a dependency on microscale properties. $(.)_{,i}$ denotes the spatial gradient of any field along the ith direction. Owing to the Y-periodicity of the material, the thermal conductivity tensor has the following property:

$$\kappa_{ij}^{\varepsilon}(\mathbf{x} + \mathbf{Y}) = \kappa_{ij}^{\varepsilon}(\mathbf{x}), \quad \forall \mathbf{x} \in \Omega. \tag{14}$$

Hence, it is evident that the conductivity tensor varies with the microscale variable $\mathbf{y}$, indicating that the problem's solution is influenced by both the macrolength and microlength scales. Furthermore, assuming that the periodicity of the material characteristics imposes a similar periodic perturbation on factors governing the thermal behavior of the material, a two-scale asymptotic expansion of the solution $T(\mathbf{x})$ shall be considered in terms of both macrovariables and microvariables.

$$T^{\varepsilon}(\mathbf{x}) = T_0(\mathbf{x}, \mathbf{y}) + \varepsilon T_1(\mathbf{x}, \mathbf{y}) + \varepsilon^2 T_2(\mathbf{x}, \mathbf{y}). \tag{15}$$

Similar expansion with respect to powers of ε can be written for temperature gradient and heat flux.

From the governing equations, using relations (10) and (11) in Eq. (9), we get

$$-(\kappa_{ij}^{\varepsilon}(\mathbf{x})T_{,j})_{,i} = 0. \tag{16}$$

Given Eq. (16), in order to determine temperature field asymptotes, the chain rule is exploited as follows:

$$T_{,i} = T_{,i(x)} + \frac{1}{\varepsilon}T_{,i(y)}. \tag{17}$$

Making use of Eqs. (17) and (15), we get Eq. (16) to be expanded as

$$
\begin{aligned}
&-\left(\kappa_{ij}(\mathbf{y})T_{0_{,j(x)}}\right)_{,i(x)} - \frac{1}{\varepsilon}\left(\kappa_{ij}(\mathbf{y})T_{0_{,j(x)}}\right)_{,i(y)} \\
&-\frac{1}{\varepsilon}\left(\kappa_{ij}(\mathbf{y})T_{0_{,j(y)}}\right)_{,i(x)} - \frac{1}{\varepsilon^2}\left(\kappa_{ij}(\mathbf{y})T_{0_{,j(y)}}\right)_{,i(y)} \\
&-\varepsilon\left(\kappa_{ij}(\mathbf{y})T_{1_{,j(x)}}\right)_{,i(x)} - \left(\kappa_{ij}(\mathbf{y})T_{1_{,j(x)}}\right)_{,i(y)} \\
&-\left(\kappa_{ij}(\mathbf{y})T_{1_{,j(y)}}\right)_{,i(x)} - \frac{1}{\varepsilon}\left(\kappa_{ij}(\mathbf{y})T_{1_{,j(y)}}\right)_{,i} = 0.
\end{aligned}
\tag{18}
$$

Grouping the results in $\mathcal{O}(\varepsilon)$, the leading order terms are given by

$$-\left(\kappa_{ij}(\mathbf{y})V_{0_{,j(y)}}\right) = 0. \tag{19}$$

For a solution to exist, Eqs. (19) and (20) must satisfy the solvability condition.[6] Equation (19) inherently fulfills the solvability condition, implying that T_0 is solely a function of the macroscopic variable $\mathbf{x}$. By grouping the next order terms in ε, we obtain

$$-\left(\kappa_{ij}(\mathbf{y})T_{0_{,j(x)}}\right)_{,i(y)} - \left(\kappa ij(\mathbf{y})T_{1_{,j(y)}}\right)_{,i(y)} = 0. \tag{20}$$

For Eq. (20) to satisfy the solvability condition, the solution T_1 takes the form

$$T_1(\mathbf{x}, \mathbf{y}) = Z_j(\mathbf{y})T_{0_{,j(x)}}, \tag{21}$$

where Z represents the homogenization function, which exhibits periodicity with a period of Y. The zero-order component of the equation of heat balance (16), considering Eqs. (20) and (21), yields the governing equation or the cell problem, which must be solved to determine Z.

$$-\left(\kappa_{ij}(\mathbf{y}) + \kappa_{ik}(\mathbf{y})Z_{j,k(y)}(\mathbf{y})\right)_{,i(y)} = 0. \quad (22)$$

The volumetric average of a quantity a over Y is defined by

$$a^H = \frac{1}{|Y|}\int_Y a(\mathbf{x},\mathbf{y})\,dY. \quad (23)$$

Using the results from Eqs. (9), (15), and (23), The macro-behavior can be defined now by averaging the terms in Eq. (22), in the domain Y. The heterogeneous structure can now be studied as a homogeneous one, with the effective conductivity κ^H given by

$$\kappa_{ij}^H = \frac{1}{|Y|}\int_Y \left(\kappa ij(\mathbf{y}) + \kappa_{ik}(\mathbf{y})Z_j(\mathbf{y})_{,k(y)}\right)dY. \quad (24)$$

B. Numerical implementation method

The cell problem derived from AHM as defined by Eq. (22) can be solved numerically using FE.[59] To predict the effective conductivity matrix, a unit potential is applied in x, y, and z directions, resulting in three distinct solutions for the homogenization function. The homogenization function Z within a given element can then be expressed in matrix form as

$$[Z(\mathbf{y})] = \begin{bmatrix} Z^{f_1} & Z^{f_2} & Z^{f_3} \end{bmatrix}_{1\times 3}, \quad (25)$$

where Z^{f_i} is the solution of cell problem for the applied unit potential difference along the direction y_i. The ($\sim$) in the following expression denotes the nodal value matrix in a finite element mesh of the unit cell, corresponding to the applied unit potential difference along with y_i. We have the usual representations for each element as

$$[\mathbf{Z}(\mathbf{y})]_{1\times 3} = [\mathbf{N}(\mathbf{y})]_{1\times n}\{\tilde{Z}\}_{n\times 3}, \quad (26)$$

where $[\mathbf{N}]$ is the matrix of the standard Lagrange shape functions and n is the number of degrees of freedom per element. The variational form of Eq. (22) can be given as

$$\int_Y \left(\kappa_{ij}(\mathbf{y}) + \kappa_{ik}(\mathbf{y})Z_{j,k}(\mathbf{y})\right)\nu_{,j}\,dY = 0, \quad (27)$$

where ν is the variation in Z. Using the matrix notations for FE, the variational form can be rewritten as

$$\int_Y \left([B]^T[D] + [B]^T[D][B]\{\tilde{Z}\}\right)dY = 0. \quad (28)$$

The system of linear equations that is to be solved reduces to

$$[K]\{\tilde{Z}\} + \{F\} = \{0\}, \quad (29)$$

where Z is Y-periodic with zero mean value over the unit cell, and

$$\{F\} = \int_Y [B]^T[D]\,dY, \quad [K] = \int_Y [B]^T[D][B]\,dY,$$
$$[B]_{3\times n} = [L]_{3\times 1}[N]_{1\times n}.$$

where L denotes the matrix of differential operators, and D denotes the coefficient of thermal conductivity of the corresponding element. Having calculated Z and by the consequence T_1, the effective material conductivity can therefore be derived as

$$\kappa_{ij}^H = \frac{1}{|Y|}\int_Y [D]\left([I] + [B]\{\tilde{Z}\}\right)dY. \quad (30)$$

In-house Python codes were developed to compute the effective conductivity as given by Eq. (30). The code was initially benchmarked for a solid spherical inclusion and then expanded to accommodate core-shell inclusions for a range of volume fractions and conductivity ratios.

IV. RESULTS AND DISCUSSION
A. Spherical inclusion

In this section, to validate the proposed model, we employ a core-shell inclusion model with core-shell inclusions arranged in a simple cubic structure within a matrix, as depicted in Fig. 4(a). For initial validation, we assume equal thermal conductivities for both the core and shell phases, enabling direct comparison with two-phase models across all volume fractions up to the maximum packing fraction characteristic of the simple cubic arrangement. We define κ_c as the conductivity of the core, κ_s as the conductivity of the shell, and κ_m as the conductivity of the matrix. The conductivity of the core-shell inclusion phase is indicated by κ_{csp}, and the conductivity ratio is indicated by $\kappa_r = \kappa_{csp}/\kappa_m$. For the simulations, we assume isotropic conductivities for all phases.

A mesh convergence study was carried out for each volume fraction of inclusion until the difference between the effective property calculated for the current mesh and the subsequent finer mesh was less than a specified tolerance value (10^{-2}), as suggested in the literature.[60] The simulations were carried out for two conductivity ratios $\kappa_r = 10^2, 10^4$. Based on Fig. 4(b), it was determined that 190 000 four-noded tetrahedral elements at a volume fraction $\phi_{csp} = 0.5$ and $\kappa_r = 10^4$ were sufficient for this simulation.

Figure 5(a) presents a comparison between our model and existing analytical estimates. At lower volume fractions ($\phi_{csp} < 0.1$), our results align closely with the Maxwell model, which is expected due to the weak interactions between inclusions in dilute systems. However, as the volume fraction increases and approaches the maximum packing fraction ($\phi_{csp} > 0.5$), there are noticeable deviations. This divergence arises because Maxwell's mean-field model does not account for significant interactions between neighboring particles, which impact the effective properties of the material. Unlike the Maxwell model, the Asymptotic Homogenization Method incorporates field perturbations caused by these inclusions [as shown in Eq. (20)], allowing it to provide more accurate predictions, especially at high-volume fractions near the maximum packing limit.

Figure 5(b) illustrates the accuracy of the asymptotic homogenization method by comparing its predictions in two conductivity ratios with Keller's results and the limit defined by Sangani and Acrivos at the maximum packing fraction ($\phi_{max} = 0.52$ for a simple cubic structure). The AHM results are in close agreement with Keller's predictions and fall within the bounds established by Sangani and Acrivos, demonstrating the validity and feasibility of the proposed approach. These results for spherical core-shell structures with equal thermal conductivities, are consistent with foundational work on the effective conductivity of spherical inclusions.

B. Core-shell inclusion

In this section, we analyze the thermal properties of composites with spherical core-shell inclusions, where the core and shell possess distinct thermal conductivities, κ_c and κ_s, respectively.
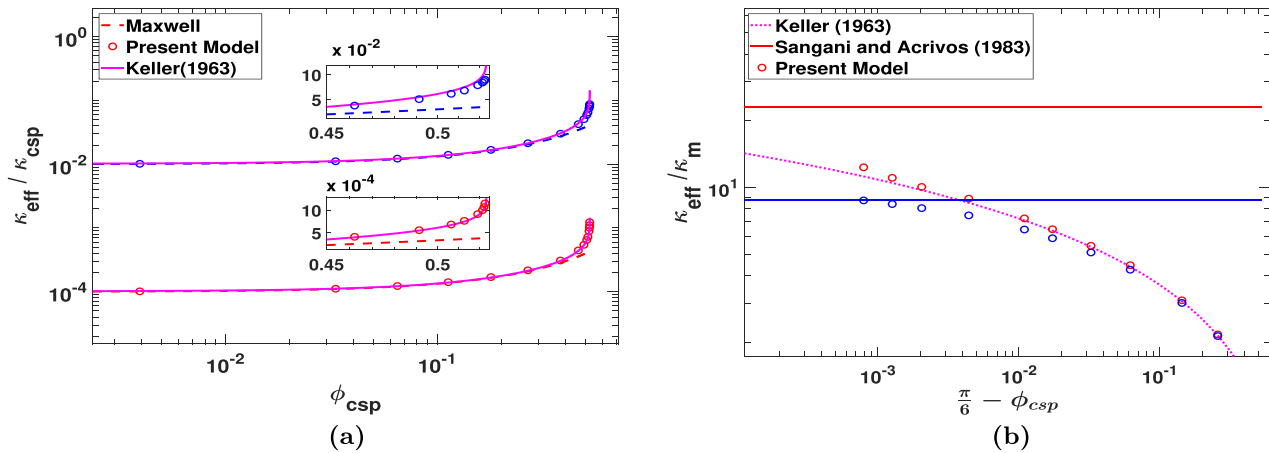
FIG. 5. (a) The ratio of $\kappa_{eff}/\kappa_{csp}$ as a function of the inclusion's volume fraction ϕ_{csp}. The dashed line corresponds to Maxwell's model, whereas the dotted line represents Keller's result. The results from the present model are plotted using circles. (b) The ratio of κ_{eff}/κ_m as a function of the deviation from the maximum packing fraction $\pi/6$ (simple cubic arrangement of spherical inclusions). The dotted line corresponds to Keller's expression, while the solid lines represent the limits predicted by Sangani and Acrivos at the maximum packing fraction. The values obtained for conductivity ratios $\kappa_r = 10^2$ and 10^4 are represented by blue and red color, respectively.

The Felske[27] model provides an analytical solution for estimating the effective thermal conductivity of composites with concentric core-shell structures, accounting for the distinct thermal properties of the core and shell materials. While this model addresses individual core-shell inclusions, it does not fully capture interactions between inclusions, which can be significant at higher volume fractions. In contrast, Lu and Song[29] employed a boundary value problem approach using twin spherical expansions to account for interactions between pairs of coated spheres in a composite material. Their rigorous method captures the field perturbations caused by neighboring inclusions, providing more accurate predictions for effective thermal conductivity in systems where particle interactions play a critical role.

In Fig. 6, the AHM model results are compared with the predictions of Lu and Song, as well as the Felske model. At lower volume fractions, both the AHM model and the Felske model show similar

results, reflecting their ability to accurately predict effective thermal conductivity in dilute conditions where particle interactions are minimal. However, as the volume fraction increases, the AHM model diverges from the Felske model and aligns more closely with the predictions of Lu and Song. This is particularly evident at non-dilute volume fractions, where particle interactions become significant. The AHM model effectively captures the influence of these interactions, demonstrating consistency with the behavior observed in Lu and Song's results. This close alignment validates the AHM model's capability to accurately account for complex particle interactions, making it a reliable tool for predicting thermal properties in core-shell composites at higher inclusion concentrations.

1. Effect of core and shell thermal conductivites

Figure 7 illustrates the effective thermal conductivity predicted by the AHM and Felske models at two different volume fractions. At a lower volume fraction [$\phi_{csp} = 0.2$, Fig. 7(a)], both models align closely and accurately predict the ETC. However, at a higher volume fraction [$\phi_{csp} = 0.5$, Fig. 7(b)], particularly when $\kappa_s/\kappa_m \gg 1$, the numerical results from the AHM model begin to deviate from the Felske model. This deviation indicates that the Felske model underestimates the effective thermal conductivity of core-shell composites at high volume fractions.

Both the core and shell significantly influence the effective conductivity, but their effects vary depending on the thermal conductivities of each component. When the ratio of the conductivity of the shell-to-matrix is extremely high ($\kappa_s/\kappa_m = 10^3$ and $\kappa_s/\kappa_m = 10^{-3}$), the effective conductivity of the composite remains largely unchanged regardless of the core-to-matrix conductivity ratio. This highlights that the effective conductivity is primarily governed by the shell conductivity, with the core exerting a limited impact.

2. Effect of spatial distribution of the inclusions

Although the periodicity assumption simplifies the analysis of composite materials, it is crucial to understand that actual composites
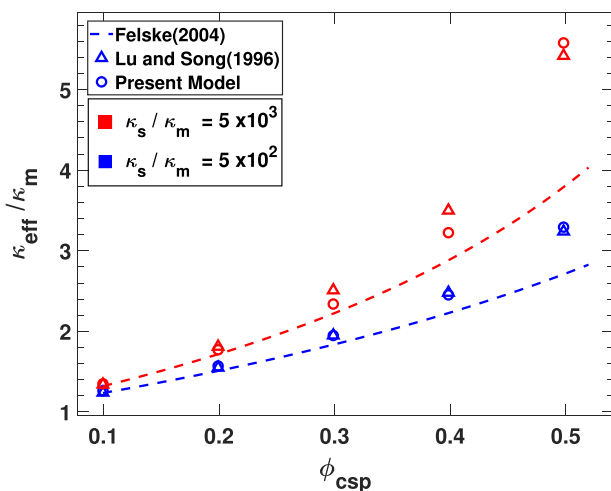

FIG. 6. Ratio of κ_{eff}/κ_m as a function of the inclusion's volume fraction ϕ_{csp} for $\kappa_c/\kappa_m = 0.01°$.
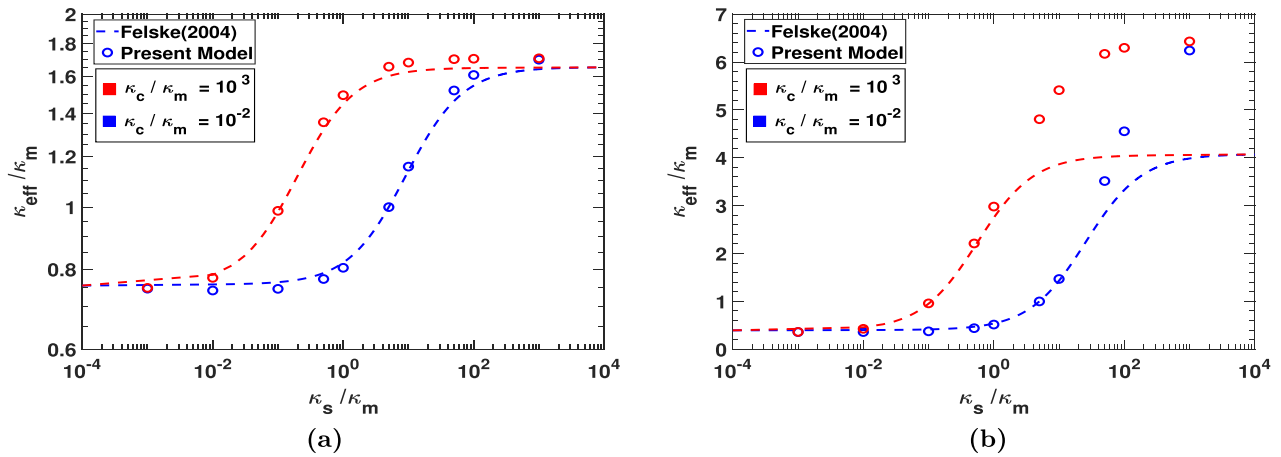
FIG. 7. Ratio of κ_{eff}/κ_m as a function of the conductivity ratio κ_s/κ_m　(a) $\phi_{csp} = 0.2°$ and (b) $\phi_{csp} = 0.5$. The x axis is displayed on a logarithmic scale for enhanced clarity.

frequently differ from this idealized model. In practice, composites exhibit a more intricate microstructure, often featuring clusters or networks of particles. The presence of particle agglomerations or network formations can significantly alter the thermal conduction pathways, thereby affecting the material's overall heat transfer characteristics. These clusters can have a substantial impact on the effective thermal conductivity of the composite. To extend the analysis, we consider computational cells where inclusions are arranged in random dispersions, as shown in Fig. 8. The macroscopic composite is modeled as a periodic array of these cells, each containing randomly placed inclusions. The Latin hypercube sampling (LHS)[61] technique is used to ensure a structured, yet random distribution of inclusions within each cubic cell. This method ensures that inclusions are evenly distributed throughout the cell without overlapping, while maintaining randomness.

In ABAQUS, a core-shell composite is constructed as follows:

1. The core radius (R_c), core-shell radius ratio (R_c/R_s), and the number of particles (N) required for a specific volume ratio (ϕ_{csp}) are determined.
2. Core-shell particles are randomly placed in a 3D cubic domain using coordinates generated by the LHS technique. The position of each new particle is checked to prevent overlap with existing particles. If an overlap occurs, the coordinate is discarded.
3. The process is repeated until the required number of particles is placed without overlap.
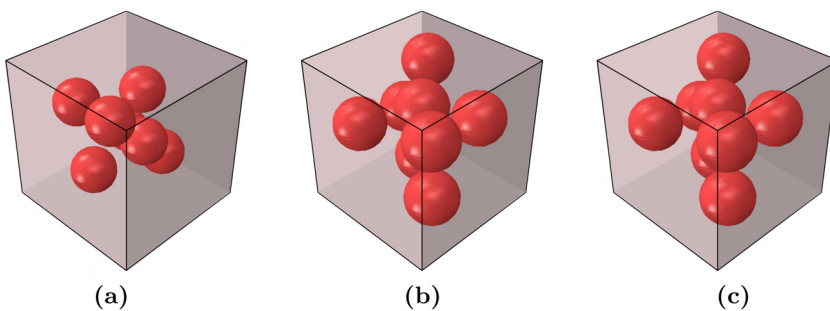
The computational model for this simulation consists of a unit cell that contains eight particles. The simulations were conducted with a core-to-shell radius ratio of $R_c/R_s = 0.9$. The effects of varying volume fractions were investigated by systematically increasing the size of the inclusions, thus increasing the overall volume fraction in the composite. Three specific volume fractions are analyzed, as depicted in Fig. 8. The thermal conductivities for the core, shell and matrix materials are established at $\kappa_c = 0.24 \, \text{W·m}^{-1}\text{·K}^{-1}$, $\kappa_s = 430 \, \text{W·m}^{-1}\text{·K}^{-1}$, and $\kappa_m = 0.45 \, \text{W·m}^{-1}\text{·K}^{-1}$, respectively. These values correspond to composite silver-coated polyamide inclusions embedded within a high-density polyethene (HDPE) matrix.[32]

As shown in Fig. 9, two different inclusion configurations are illustrated: (a) a simple cubic arrangement and (b) a randomly oriented arrangement. The results presented in Table II indicate that the effective thermal conductivity κ_{eff} of the composite increases with the volume fraction of inclusions. In addition, comparing computational cells with a periodic arrangement of inclusions to those with a random arrangement, the latter demonstrates a significant increase in κ_{eff}. The findings reveal that particle interactions and collective effects gain prominence in the semidilute volume fraction regime, leading to a marked increase in effective thermal conductivity. As the volume fraction increases, the interaction of the particles intensifies, leading to enhanced effective thermal conductivity.

The observed enhancement in effective thermal conductivity can be attributed to several factors inherent in the random arrangement of
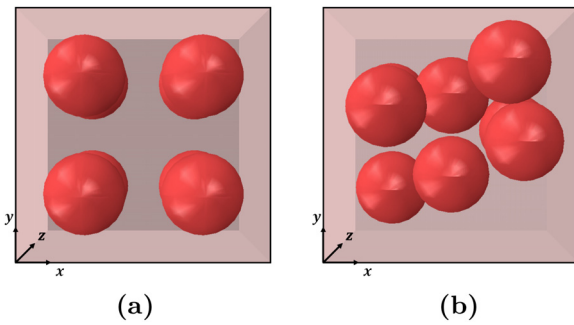

(a)　　　　　(b)　　　　　(c)

FIG. 8. Computational cells containing monodisperse core-shell inclusions with $R_c/R_s = 0.9$ and (a) $\phi_{csp} = 0.11$, (b) $\phi_{csp} = 0.18$, and (c) $\phi_{csp} = 0.26$.

FIG. 9. Computational cell with (a) inclusions arranged in a simple cubic lattice within the unit cell, and (b) inclusions with random orientations that show a preferential alignment along the x axis at $\phi_{csp} = 0.26$.

the particles. First, this configuration allows for multiple conduction pathways, thereby increasing conductivity across all directions. Additionally, as illustrated in Fig. 9(b), random orientations can include preferential alignments, such as along the x axis, which further enhance thermal conduction in that specific direction. This directional enhancement is evident in the results for $\phi_{csp} = 0.26$ shown in Table II, where the effective conductivity is higher along the **x** direction compared to the **y** and **z** directions. This pattern suggests that alignments along certain axes lead to improved conduction along those paths, contributing to an overall increase in κ_{eff}. Furthermore, the relative spread of the ETC at moderate volume fractions is higher than at close packing. This can be attributed to the wide range of possible spatial arrangements and conduction paths between inclusions at moderate volume fractions. In contrast, the particles are more densely packed in the near-packing limit, restricting their rearrangement and resulting in a smaller spread of ETC values.

3. Comparison with experimental results

Numerous experimental[32–34] studies have measured the effective thermal conductivity of three-component core-shell composites. These measurements were compared with theoretical models such as

TABLE II. Numerical predictions of the effective thermal conductivity for composites with inclusions arranged periodically (SC) and randomly distributed within a computational cell.

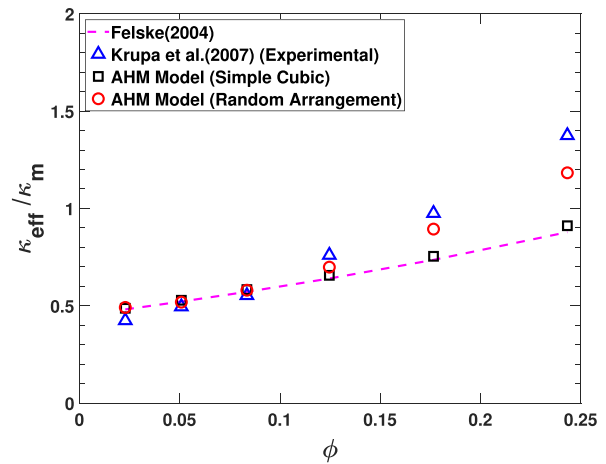|		κ_{eff} (W/mK)		
ϕ_{csp}	Direction	SC	Random	% difference
	x	0.62	0.67	7.56
0.11	y	0.62	0.69	11.19
	z	0.62	0.68	10.34
	x	0.74	0.83	10.28
0.18	y	0.74	0.84	13.14
	z	0.74	0.87	15.89
	x	0.95	1.13	19.09
0.26	y	0.95	1.04	8.84
	z	0.95	1.08	13.75

FIG. 10. Comparison of effective thermal conductivity predicted from theoretical and numerical models with experimental results.

Felske[27] and numerical models. Numerical studies, such as those conducted by Thiele et al.,[26] have applied finite element methods for estimating thermal conductivity; however, they often do not fully account for particle orientation and interaction effects, which are crucial at higher volume fractions where these interactions significantly influence overall thermal conductivity.

As illustrated in Fig. 10, experimental data are compared with theoretical predictions from both the Felske model[27] and the AHM model with simple cubic and random arrangements. Both models show reasonable agreement with experimental results at low volume fractions, but the AHM model with random particle arrangements achieves a closer match at higher volume fractions. This improvement can be attributed to the random arrangement that brings particles closer together, enabling more interactions that enhance thermal conductivity. The random arrangement of the particles not only allows for greater interparticle interactions but also exhibits a preferential alignment along the x axis, as plotted for uniformity. This preferential orientation contributes to an increase in effective thermal conductivity, particularly in the x-direction, by supporting enhanced thermal transport along this axis. In addition, as the number of particles and the size of the unit cell increased, leading to a more randomized particle arrangement, the results showed even closer alignment with the experimental data. This trend suggests that the greater randomness and density of particles enhance the accuracy of the thermal conductivity predictions. This observation further supports the reliability of this approach in capturing complex interactions in higher volume fractions, indicating its potential for more precise thermal analysis in composite materials.

Krupa et al.[32] also mention the presence of continuous conductive chains within their samples, a factor absent in our simulations. Despite this limitation, the AHM model captures significant particle–matrix interactions, providing a reliable representation of the physical processes involved in the thermal behavior of core-shell composites.

V. CONCLUSION

The asymptotic homogenization method coupled with finite element analysis has demonstrated its effectiveness in predicting the

thermal behavior of composites with core-shell inclusions. This study highlights how critical factors such as the volume fraction of inclusions, the thermal conductivity of the shell, and particle orientation play a pivotal role in determining the effective thermal conductivity of these materials. The analysis revealed that the thermal conductivity of the shell material plays a decisive role, and applying a conductive coating can significantly improve the overall thermal performance by facilitating better heat transfer between particles and the matrix. Furthermore, the arrangement and orientation of the particles significantly affect the ETC, underscoring the importance of microstructural considerations when designing composites for thermal applications.

The approach used in this study not only aligns with traditional models but also provides a more detailed understanding of deviations arising from particle interactions, especially in moderate and dense packing scenarios. The adaptability of this method for diverse configurations and inclusion types extends its potential applications, offering valuable insights for optimizing thermal performance in advanced composite materials.

ACKNOWLEDGMENTS

AUTHOR DECLARATIONS
Conflict of Interest

The authors have no conflicts to disclose.

Author Contributions

A. Karthiban: Formal analysis (equal); Investigation (equal); Methodology (equal); Writing – original draft (equal); Writing – review & editing (equal). **M. K. Easwar:** Methodology (equal); Validation (equal); Writing – original draft (equal); Writing – review & editing (equal). **A. Arockiarajan:** Conceptualization (equal); Resources (lead); Supervision (equal); Validation (equal); Writing – review & editing (equal). **Anubhab Roy:** Conceptualization (equal); Resources (lead); Supervision (equal); Validation (equal); Writing – review & editing (equal).

DATA AVAILABILITY

The data that support the findings of this study are available from the corresponding author upon reasonable request.

REFERENCES

[1]H. K. Azad and D. Rahman, "Ceramic matrix composites with particulate reinforcements—progress over the past 15 years," in *Comprehensive Materials Processing* (Elsevier, 2024), pp. 395–408.

[2]N. P. Chuan-Yong Zhu and Z.-Y. Li, "Design and thermal insulation performance analysis of endothermic opacifiers doped silica aerogels," Int. J. Therm. Sci. **145**, 105995 (2019).

[3]H. Chen, V. V. Ginzburg, J. Yang, Y. Yang, W. Liu, Y. Huang, L. Du, and B. Chen, "Thermal conductivity of polymer-based composites: Fundamentals and applications," Prog. Polym. Sci. **59**, 41–85 (2016).

[4]T. Mori and K. Tanaka, "Average stress in matrix and average elastic energy of materials with misfitting inclusions," Acta Metall. **21**, 571 (1973).

[5]R. Hill, "A self-consistent mechanics of composite materials," J. Mech. Phys. Solids **13**, 213 (1965).

[6]G. Papanicolau, A. Bensoussan, and J.-L. Lions, *Asymptotic Analysis for Periodic Structures* (Elsevier, 1978).

[7]N. Charalambakis, "Homogenization techniques and micromechanics. A survey and perspectives," Appl. Mech. Rev. **63**, 030803 (2010).

[8]Maxwell, J., *A Treatise on Electricity and Magnetism* (Clarendon Press, 1873), Vol. 1.

[9]J. Keller, "Conductivity of a medium containing a dense array of perfectly conducting spheres or cylinders or nonconducting cylinders," J. Appl. Phys. **34**, 991 (1963).

[10]G. K. Batchelor and R. W. O'Brien, "Thermal or electrical conduction through a granular material," Proc. R. Soc. Lond. A **355**, 313–333 (1977).

[11]R. C. McPhedran and D. R. McKenzie, "The conductivity of lattices of spheres. i. the simple cubic lattice," Proc. R. Soc. Lond. A **359**, 45–63 (1978).

[12]A. S. Sangani and A. Acrivos, "The effective conductivity of a periodic array of spheres," Proc. R. Soc. Lond. A **386**, 263–275 (1983).

[13]M. Zuzovsky and H. Brenner, "Effective conductivities of composite materials composed of cubic arrangements of spherical particles embedded in an isotropic matrix," J. Appl. Math. Phys. **28**, 979–992 (1977).

[14]E. M. K, A. Arockiarajan, and A. Roy, "A multiscale approach to predict the effective conductivity of a suspension using the asymptotic homogenization method," Phys. Fluids **34**, 062002 (2022).

[15]T. Nomura, N. Sheng, C. Zhu, G. Saito, D. Hanzaki, T. Hiraki, and T. Akiyama, "Microencapsulated phase change materials with high heat capacity and high cyclic durability for high-temperature thermal energy storage and transportation," Appl. Energy **188**, 9–18 (2017).

[16]Y. Zhu, S. Liang, K. Chen, X. Gao, P. Chang, C. Tian, J. Wang, and Y. Huang, "Preparation and properties of nanoencapsulated n-octadecane phase change material with organosilica shell for thermal energy storage," Energy Convers. Manag. **105**, 908–917 (2015).

[17]D. Mao, J. Chen, L. Ren, K. Zhang, M. M. Yuen, X. Zeng, R. Sun, J.-B. Xu, and C.-P. Wong, "Spherical core-shell al@al2o3 filled epoxy resin composites as high-performance thermal interface materials," Compos. Part A Appl. Sci. Manuf. **123**, 260–269 (2019).

[18]D. Hasselman and L. F. Johnson, "Effective thermal conductivity of composites with interfacial thermal barrier resistance," J. Compos. Mater. **21**, 508–515 (1987).

[19]G. Sukhinin, M. Morozova, and S. Novopashin, "Thermal conductivity of the suspensions based on core-shell particles," J. Heat Transfer **138**, 064501 (2016).

[20]E. Herve, "Thermal and thermoelastic behaviour of multiply coated inclusion-reinforced composites," Int. J. Solids Struct. **39**, 1041–1058 (2002).

[21]Y. K. Park, J.-K. Lee, and J.-G. Kim, "A new approach to predict the thermal conductivity of composites with coated spherical fillers and imperfect interface," Mater. Trans. **49**, 733–736 (2008).

[22]W. Woodside and J. H. Messmer, "Thermal conductivity of porous media. I. Unconsolidated sands," J. Appl. Phys. **32**, 1688–1699 (1961).

[23]K. Lichtenecker, "Die dielektrizitatskonstante naturlicher und kunstlicher mischkorper," Physikalische Z. **27**, 115–158 (1926).

[24]A. D. Brailsford and K. G. Major, "The thermal conductivity of aggregates of several phases, including porous materials," Br. J. Appl. Phys. **15**, 313 (1964).

[25]I. L. Ngo and V. A. Truong, "An investigation on effective thermal conductivity of hybrid-filler polymer composites under effects of random particle distribution, particle size and thermal contact resistance," Int. J. Heat Mass Transf. **144**, 118605 (2019).

[26]A. M. Thiele, A. Kumar, G. Sant, and L. Pilon, "Effective thermal conductivity of three-component composites containing spherical capsules," Int. J. Heat Mass Transf. **73**, 177–185 (2014).

[27]J. Felske, "Effective thermal conductivity of composite spheres in a continuous medium with contact resistance," Int. J. Heat Mass Transf. **47**, 3453–3461 (2004).

[28]R. Pal, "Thermal conductivity of three-component composites of core-shell particles," Mater. Sci. Eng. A **498**, 135–141 (2008).

[29]S. Lu and J. Song, "Effective conductivity of composites with spherical inclusions: Effect of coating and detachment," J. Appl. Phys. **79**, 609–618 (1996).

[30]Y. C. Chiew and E. D. Glandt, "Effective conductivity of dispersions: The effect of resistance at the particle surfaces," Chem. Eng. Sci. **42**, 2677–2685 (1987).

[31]Z. Shen and H. Zhou, "Predicting effective thermal and elastic properties of cementitious composites containing polydispersed hollow and core-shell microparticles," Cem. Concr. Compos. **105**, 103439 (2020).

[32]I. Krupa, A. Boudenne, and L. Ibos, "Thermophysical properties of polyethylene filled with metal coated polyamide particles," Eur. Polym. J. **43**, 2443–2452 (2007).

[33]Z. Wang, Y. Zhang, J. Yi, N. Cai, and J. Guo, "Core-shell cu@al2o3 fillers for enhancing thermal conductivity and retaining electrical insulation of epoxy composites," J. Alloys Compd. **928**, 167123 (2022).

[34]H. Wang, F. Hou, and C. Chang, "Experimental and computational modeling of thermal conductivity of cementitious syntactic foams filled with hollow glass microspheres," Constr. Build. Mater. **265**, 120739 (2020).

[35]Y. Qiao, X. Wang, X. Zhang, and Z. Xing, "Thermal conductivity and compressive properties of hollow glass microsphere filled epoxy-matrix composites," J. Reinf. Plast. Compos. **34**, 1413 (2015).

[36]A. Ricklefs, A. M. Thiele, G. Falzone, G. Sant, and L. Pilon, "Thermal conductivity of cementitious composites containing microencapsulated phase change materials," Int. J. Heat Mass Transf. **104**, 71–82 (2017).

[37]Y. Zhou, L. Wang, H. Zhang, Y. Bai, Y. Niu, and H. Wang, "Enhanced high thermal conductivity and low permittivity of polyimide based composites by core-shell Ag@SiO$_2$ nanoparticle fillers," Appl. Phys. Lett. **101**, 012903 (2012).

[38]K. Zheng, D. Wang, L. Duo, F. Sun, Z. Zhang, Y. He, P. Li, Y. Ma, and C. Xu, "Covalently bonded silica interfacial layer for simultaneously improving thermal and dielectric performance of copper/epoxy composite," Surf. Interfaces **26**, 101404 (2021).

[39]H. Hatta and M. Taya, "Thermal conductivity of coated filler composites," J. Appl. Phys. **59**, 1851–1860 (1986).

[40]R. T. Bonnecaze and J. F. Brady, "A method for determining the effective conductivity of dispersions of particles," Proc. R. Soc. Lond. A **430**, 285–313 (1990).

[41]C.-W. Nan, R. Birringer, D. R. Clarke, and H. Gleiter, "Effective thermal conductivity of particulate composites with interfacial thermal resistance," J. Appl. Phys. **81**, 6692–6699 (1997).

[42]Y. Benveniste and G. W. Milton, "An effective medium theory for multi-phase matrix-based dielectric composites with randomly oriented ellipsoidal inclusions," Int. J. Eng. Sci. **49**, 2–16 (2011).

[43]H. Cheng and S. Torquato, "Effective conductivity of periodic arrays of spheres with interfacial resistance," Proc. R Soc. Lond. A **453**, 145–161 (1997).

[44]C.-Y. Zhu, W.-X. Yang, H.-B. Xu, B. Ding, L. Gong, and Z.-Y. Li, "A general effective thermal conductivity model for composites reinforced by non-contact spherical particles," Int. J. Therm. Sci. **168**, 107088 (2021).

[45]S. Torquato, "Random heterogeneous media: Microstructure and improved bounds on effective properties," Appl. Mech. Rev. **44**(2): 37–76 (1991).

[46]E. Andreassen and C. S. Andreasen, "How to determine composite material properties using numerical homogenization," Comput. Mater. Sci. **83**, 488 (2014).

[47]F. Fantoni, A. Bacigalupo, and M. Paggi, "Multi-field asymptotic homogenization of thermo-piezoelectric materials with periodic microstructure," Int. J. Solids Struct. **120**, 31 (2017).

[48]T. A. Dutra, R. T. L. Ferreira, H. B. Resende, A. Guimarães, and J. M. Guedes, "A complete implementation methodology for asymptotic homogenization using a finite element commercial software: Preprocessing and postprocessing," Compos. Struct. **245**, 112305 (2020).

[49]D. Lee and J. Lee, "Comparison and validation of numerical homogenization based on asymptotic method and representative volume element method in thermal composites," Multiscale Sci. Eng. **3**, 165 (2021).

[50]P. Suquet, "Elements of homogenization for inelastic solid mechanics, homogenization techniques for composite media," in *Homogenization Techniques for Composite Media*, edited by E. Sanchez-Palencia and A. Zaoui (Springer, Berlin, 1987), pp. 193–279.

[51]S. Torquato, *Random Heterogeneous Materials: Microstructure and Macroscopic Properties* (Springer, 2002), Vol. 55, pp. B62–B63.

[52]P. Kanoute, D. Boso, J. Chaboche, and B. Schrefler, "Multiscale methods for composites: A review," Arch. Comput. Methods Eng. **16**, 31 (2009).

[53]A. L. Kalamkarov, I. V. Andrianov, and V. V. Danishevs'kyy, "Asymptotic homogenization of composite materials and structures," Appl. Mech. Rev. **62**, 030802 (2009).

[54]J. Castillero, J. Otero, R. Ramos, and A. Bourgeat, "Asymptotic homogenization of laminated piezocomposite materials," Int. J. Solids Struct. **35**, 527 (1998).

[55]J. Bravo-Castillero, R. Rodríguez-Ramos, H. Mechkour, J. A. Otero, and F. J. Sabina, "Homogenization of magneto-electro-elastic multilaminated materials," Q. J. Mech. Appl. Math. **61**, 311 (2008).

[56]J. Bravo-Castillero, H. Mechkour, J. Otero, J. Cabanas, L. Sixto, R. G. Díaz, and F. Sabina, "Homogenization and effective properties of periodic thermomagnetoelectroelastic composites," J. Mech. Mater. Struct. **4**, 819 (2009).

[57]H. Berger, S. Kari, U. Gabbert, R. Rodriguez-Ramos, R. Guinovart, J. A. Otero, and J. Bravo-Castillero, "An analytical and numerical approach for calculating effective material coefficients of piezoelectric fiber composites," Int. J. Solids Struct. **42**, 5692–5714 (2005).

[58]S. Li and E. Sitnikova, "An excursion into representative volume elements and unit cells," in *Reference Module in Materials Science and Materials Engineering*, edited by P. W. Beaumont and C. H. Zweben (Elsevier 2017), pp. 451–489.

[59]R. L. T. Olek and C. Zienkiewicz, *The Finite Element Method for Solid and Structural Mechanics* (Butterworth-Heinemann, 2005).

[60]R. Penta and A. Gerisch, "Investigation of the potential of asymptotic homogenization for elastic composites via a three-dimensional computational study," Comput. Visual. Sci. **17**, 185 (2015).

[61]M. Mckay, R. Beckman, and W. Conover, "A comparison of three methods for selecting vales of input variables in the analysis of output from a computer code," Technometrics **21**, 239–245 (1979).

11 January 2025 07:12:38